Proceedings of the XXXIII International School of Semiconducting Compounds, Jaszowiec 2004

Investigation of Photoelectric Properties of ZnSe:Cr and ZnTe:V:Al by Picosecond Four-Wave Mixing Technique

A. Kadys[a], M. Sudzius[a], K. Jarasiunas[a,*], V. Ivanov[b], M. Godlewski[b,c] and J.-C. Launay[d]

[a]Department of Semiconductor Optoelectronics
Institute of Materials Science and Applied Research
Vilnius University, Sauletekio ave. 9 bld. 3, 10222 Vilnius, Lithuania
[b]Institute of Physics, Polish Academy of Sciences
al. Lotników 32/46, 02-668 Warsaw, Poland
[c]College of Science, Cardinal S. Wyszyński University, Warsaw, Poland
[d]Institut de Chimie de la Matière Condensée de Bordeaux (ICMCB)
33608, Pessac, France

Role of deep impurity levels in carrier generation, transport, and recombination were investigated in bulk ZnSe:Cr and ZnTe:V:Al crystals by four-wave mixing technique. The temporal and exposure dependencies of optical nonlinearities in ZnSe:Cr evidenced an influence of Cr^{1+}/Cr^{2+} states in carrier generation, exhibited very fast carrier relaxation, and revealed the presence of competing recombination mechanisms. Similar investigations in ZnTe:V:Al showed an effective carrier generation from Al-induced defect complexes as well as very fast carrier capture by Zn-vacancies.

PACS numbers: 73.50.Gr, 81.70.Fy, 61.72.Hh, 61.72.Ji

1. Introduction

Transition metal ions doped II–VI semiconductors remain very attractive materials for applications in advanced optoelectronic devices like IR and visible

*corresponding author; e-mail: kestutis.jarasiunas@ff.vu.lt

solid state lasers, terahertz-band radiation detectors, and photorefractive cells. Defect engineering of these materials requests new experimental approaches for studies of a role of deep impurities in carrier generation, transport, and recombination. In recent years, time-resolved picosecond four-wave mixing (FWM) technique has been used intensively for studies of carrier dynamics in bulk crystals and heterostructures [1–3]. An advantage of this technique, based on a detection of light-induced diffraction on nonequilibrium carrier grating, is a simple relationship between the nonlinear optical properties and photoelectric parameters of a semiconductor [4]. Previous studies of carrier transport in deep vanadium doped CdZnTe compounds [5–7] and semi-insulating GaAs [8, 9] allowed monitoring of an electrical activity of defects, their transformation under illumination, and contribution to carrier transport.

In this work, the investigation of nonequilibrium carrier dynamics in deep-impurity doped ZnSe and ZnTe crystals is reported. By measuring the temporal and exposure characteristics (EC) of light diffraction on free carrier (FC) grating, the mechanisms of carrier generation and relaxation are analyzed, and a role of deep impurities and intrinsic defects is discussed.

2. Samples and technique

Two semi-insulating bulk crystals, ZnSe:Cr and ZnTe:V:Al, were characterized by FWM technique. ZnSe:Cr crystals were obtained by physical vapor transport (PVT) method using Davydov–Markov procedure [10]. The Cr was doped at different density (from 5×10^{18} to 5×10^{19} at/cm^3) with the subsequent annealing. ZnTe:V:Al with vanadium concentration of 1.7×10^{17} at/cm^3 was grown by traveling heater method under excess tellurium and codoped by aluminum ($N_{\mathrm{Al}} = 1.5 \times 10^{19}$ at/cm^3) in order to modify the charge of deep impurity [11].

The nonequilibrium carriers were created in the crystals with $E_{\mathrm{g}} = 2.26$ eV (ZnTe) or 2.83 eV (ZnSe) using light interference pattern $I = I_0 \left[1 + \cos\left(2\pi x\right)/\Lambda\right]$

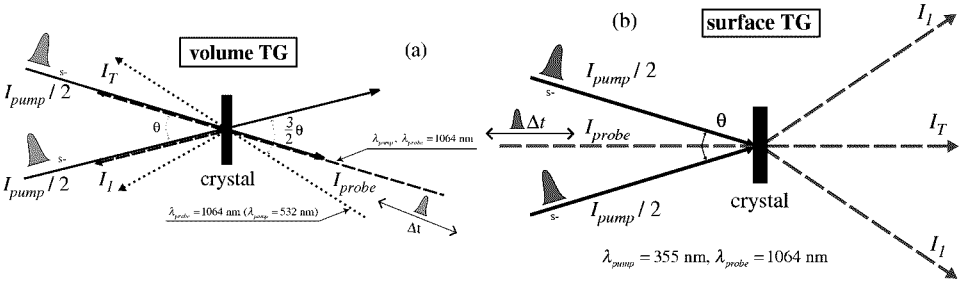

Fig. 1. Optical schemes for transient grating (TG) experiments: (a) volume gratings ($hc/\lambda_{\mathrm{pump}} < E_{\mathrm{g}}$) with probe matched to the Bragg angle for $\lambda_{\mathrm{pump}} = \lambda_{\mathrm{probe}}$ (dashed line) and $\lambda_{\mathrm{pump}} = \lambda_{\mathrm{probe}}/2$ (dotted line) cases and (b) surface gratings ($hc/\lambda_{\mathrm{pump}} > E_{\mathrm{g}}$).

of two 25 ps laser pulses. We use two wavelengths for carrier photoexcitation thus enabling deep-impurity assisted carrier generation (by quantum energy of $h\nu = 1.17$ eV in ZnTe or by 2.34 eV in ZnSe) or interband carrier generation in ZnSe by $h\nu = 3.51$ eV. In all cases, the light induced spatial modulation of carrier density $N = N_0 + \Delta N \cos(2\pi x/\Lambda)$ was monitored by light diffraction of a delayed probe beam at 1064 nm [3, 4, 12]. The corresponding optical setups are illustrated schematically in Fig. 1.

3. Results and discussion

3.1. ZnSe:Cr

At excitation of ZnSe:Cr crystals by light interference field with quantum energy $h\nu = 2.34$ eV, we observed the fast and slow decay components in light diffraction (grating decay kinetics for the sample with higher Cr concentration are shown in Fig. 2a). Nearly 5 times higher diffraction efficiency for the sample with higher Cr concentration confirmed a contribution of Cr impurity to interband carrier generation. Assuming a presence of two charge states of Cr (i.e. Cr^{1+} at 1.24 eV and Cr^{2+} at 2.2 eV below the conduction band (CB)) and that the Cr^{1+} appears only at photoexcitation [13, 14], only two-step transitions may take part in carrier generation at excitation by 532 nm wavelength. The first step is Cr^{1+} photogeneration, and the second is its photoexcitation, i.e. $Cr^{2+} + h\nu \Rightarrow Cr^{1+} + h_{VB}$ and $Cr^{1+} + h\nu \Rightarrow Cr^{2+} + e_{CB}$. In this way, Cr-assisted two-step transitions take place and produce an e–h pair.

Very fast relaxation of the conduction electrons during the action of 25 ps duration laser pulse was observed due to quite large capture cross-section of Cr^{2+} (see Fig. 2a). Moreover, a presence of long relaxation tails in the sample with higher concentration of Cr impurity ($N_{Cr} = 5 \times 10^{19}$ cm^{-3}, Fig. 2) points to the subsequent step in carrier relaxation, probably related to nonradiative recombination. Assuming that other authors have reported an efficient decrease in photoluminescence and increased Auger recombination in samples with Cr doping above 10^{19} cm^{-3} [15], we attribute the observed relaxation tail either to generation of an additional hole density via the Auger recombination, or to a local lattice heating due to fast nonradiative recombination (the latter mechanism may take place due to very high thermal lensing parameter 7×10^{-5}/K [14]). Further studies are required to determine the sign of the refractive index modulation at delay times $\Delta t > 200$ ps. At the given stage of studies, we give preference to the mechanism of temperature grating formation which is in opposite phase with respect to the free carrier grating. The opposite sign of refractive index modulations may lead to a dip in diffraction [16] if these two mechanisms are of equal strength. A weak signature of this competition is seen in Fig. 2a as the dip at $\Delta t \approx 100$ ps. On the other hand, occupation of the metastable Cr states may also result in formation

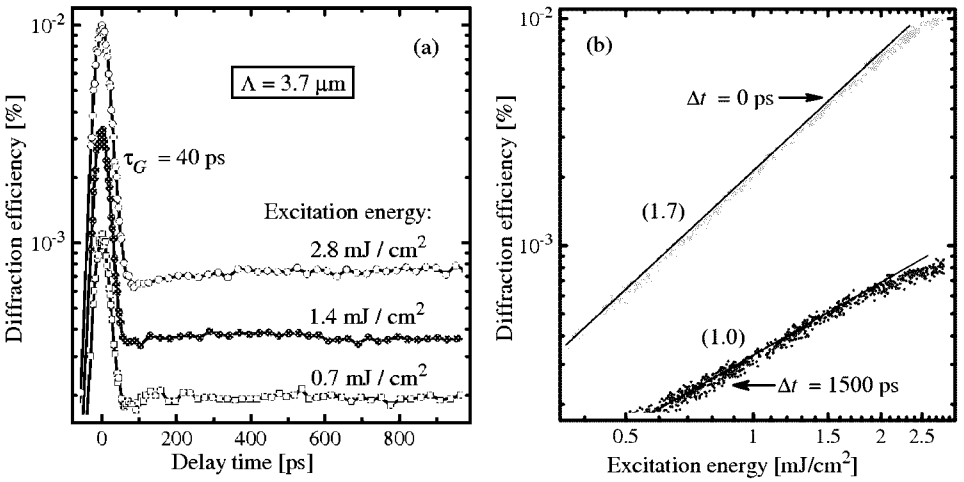

Fig. 2. Kinetics of FC grating decay (a) and exposure characteristics of diffraction efficiency (b) measured in ZnSe:Cr ($N_{\mathrm{Cr}} = 5 \times 10^{19}$ cm^{-3}) by using 534 nm wavelength light for the grating recording. Numbers in the brackets indicate the characteristic EC slopes.

of an amplitude grating and its very slow relaxation, as it was detected by FWM in GaAs:EL2 [17].

The assumption of fast nonlinear carrier recombination in ZnSe:Cr is also supported by the exposure characteristics of FC diffraction efficiency (Fig. 2b). In case of the two-step interband transitions, the power index of the dependence $\eta \propto I^{\gamma}$ would be equal to 4 (as $\eta \propto \Delta N^2$ and $\Delta N \propto I^2$ [7]). The strong and fast nonlinear recombination may diminish the carrier generation rate [3]. In the given case, the slope value $\gamma = 1.7$ points to carrier recombination mechanism of higher order than the quadratic. In addition, the exposure characteristic of the slow decay component (EC at $\Delta t = 1500$ ps, Fig. 2b) indicates its sublinear increase with excitation. Therefore, the assumption of two competing carrier recombination mechanisms is required. The hypothesis will be further analyzed on basis of numerical modeling of nonequilibrium carrier dynamics and related experimental studies of diffraction, using the tunable wavelengths of a parametric picosecond laser.

At interband carrier excitation of ZnSe:Cr ($h\nu = 3.51$ eV) due to high carrier density we managed to fill partially the fast Cr^{2+} traps and observed longer relaxation processes in diffraction kinetics (Fig. 3a): in addition to the fast component, the slower one appears with ≈ 120 ps relaxation time. Measurements at various grating periods allowed us to determine the carrier lifetime of 170 ps and the bipolar diffusion coefficient $D = 5.7$ cm^2/s (Fig. 3b). The D value is relatively large, if one assumes the carrier scattering by the ionized Cr impurity. On the other hand, the high mobility indicates the low electrical activity of Cr for this particu-

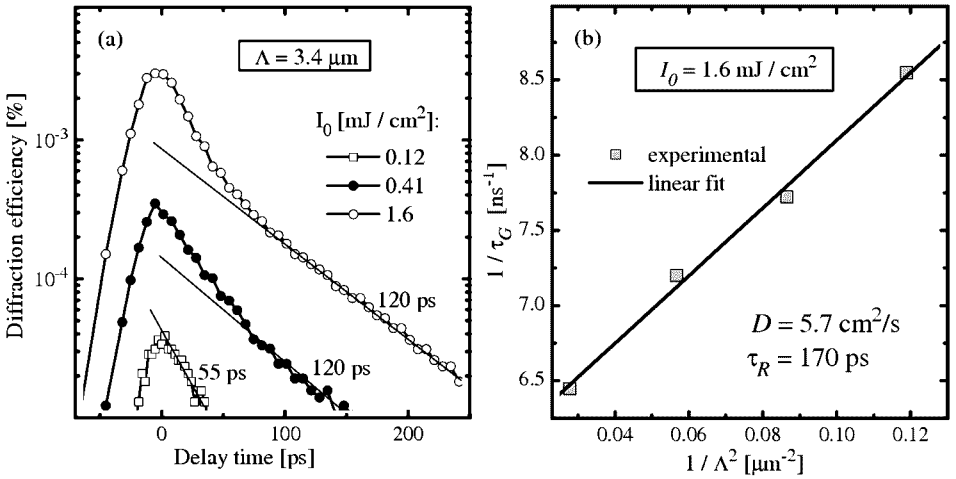

Fig. 3. Surface grating decay kinetics (a) and $1/\tau_G \propto 1/\Lambda^2$ dependence (b) measured in ZnSe:Cr ($N_{Cr} = 5 \times 10^{18}$ cm^{-3}) by using 355 nm wavelength light for the grating recording.

lar sample. Non-monotonous decay of diffraction efficiency of the surface grating recorded in ≈ 1 μm thick surface layer (Fig. 3a) requires deeper analysis based on numerical modeling in order to reveal the contribution of carrier recombination on the surface as well as nonlinear recombination in the bulk.

3.2. ZnTe:V:Al

In Fig. 4a, free carrier grating decay kinetics in ZnTe:V:Al are shown as a function of the probe delay time. The kinetics revealed fast transients at low excitations and slow relaxation tails. At higher excitations, the amplitude of fast component started to saturate. The fast transients in photocarrier dynamics are typically due to the presence of vacancies which create the acceptor-type states [5], thus the effect was attributed to Zn-vacancies in ZnTe:V:Al. We estimated the fast trap density $\Delta N_T = \Delta N$ from the saturation threshold of about $\approx 2 \times 10^{14}$ m^{-3} using the measured values of probe beam diffraction efficiency $\eta = (\pi n_{eh} \Delta N d/\lambda)^2$, where $n_{eh} \approx 2.0 \times 10^{-21}$ cm^3 is the refractive-index change per carrier pair density, calculated according to the Drude model [4].

Exposure characteristics of diffraction efficiency shown in Fig. 4b disclosed not only effective carrier recombination to the trap but also revealed sensitively the competition of one-photon and two-photon carrier generation mechanisms: at excitations below 2 mJ/cm^2 and $\Delta t = 0$ ps, the slope of EC is equal to 1.7 pointing to case of one-photon-assisted carrier generation ($\gamma = 2$) and simultaneous recombination ($\gamma < 2$). The slope coefficient increases gradually with excitation up to $\gamma = 4$ as two-photon carrier generation becomes dominant. The presence of nearly linear carrier generation channel at low excitations leads to the conclusion

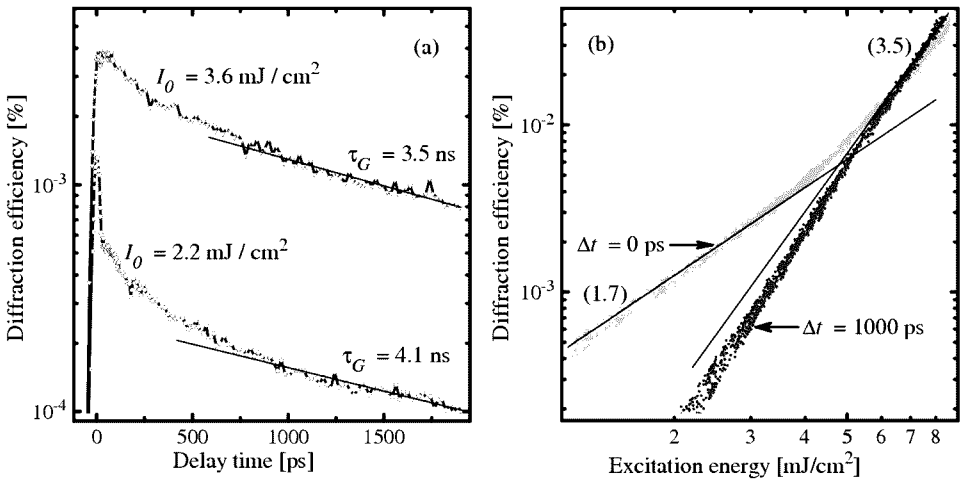

Fig. 4. Characteristics of light diffraction in ZnTe:V:Al at $\Lambda = 2.7$ μm: (a) grating kinetics at various excitation energies and (b) dependencies of diffraction efficiency shown for different delay times of the probe beam. Numbers in the brackets indicate the characteristic EC slopes.

that Al gives rise to some defect complexes with activation energy below 1.17 eV since the vanadium in ZnTe does not contribute to the electron photogeneration to CB at $h\nu = 1.17$ eV. The effect of similar origin was observed in Cl (shallow donor) codoped CdTe:V crystals [5].

4. Conclusions

Role of deep impurities in photoelectrical properties of bulk ZnSe:Cr and ZnTe:V:Al crystals were investigated by time resolved four-wave mixing technique. Cr-assisted interband carrier generation and their efficient capture by Cr^{2+} states were observed. Contribution of the additional recombination channel was suggested after analysis of slow decay components. In Al codoped ZnTe:V crystals, the fast transients in FC kinetics were attributed to simultaneous carrier generation from the codoping-induced defect complexes and the subsequent carrier capture by Zn-vacancies.

Acknowledgments

The research was sponsored by NATO's Scientific Affairs Division in the framework of the Science for Peace Programme (Project SfP-974476), European Commission (Contract No. G5MA-CT-2002-04047), and Lithuanian State Science and Studies Foundation.

References

[1] A. Miller, in: *Semiconductors and Semimetals*, Vol. 59, Eds. E. Garmire, A. Kost, Academic Press, New York 1999, p. 287.

[2] K. Jarasiunas, N. Lovergine, *Mater. Sci. Eng. B* **91-92,** 100 (2002).

[3] K. Jarasiunas, in: *UV Solid-State Light Emitters and Detectors*, Eds. M.S. Shur, A. Žukauskas, Kluwer Academic Publishers, Netherlands 2004, p. 93.

[4] R.K. Jain, M.B. Klein, in: *Optical Phase Conjugation*, Ed. R.A. Fischer, Academic Press, New York 1983, p. 307.

[5] K. Jarasiunas, L. Bastiene, J.C. Launay, P. Delaye, G. Roosen, *Semicond. Sci. Technol.* **14,** 48 (1999).

[6] K. Jarašiūnas, M. Sūdžius, R. Aleksiejūnas, K. Shcherbin, in: *Trends in Optics and Photonics Series*, Vol. 62, Eds. D.D. Nolte, G.J. Salamo, A. Siahmakoun, S. Stepanov, OSA, Washington DC 2001, p. 246.

[7] M. Sudzius, R. Aleksiejunas, K. Jarasiunas, D. Verstraeten, J.C. Launay, *Semicond. Sci. Technol.* **18,** 367 (2003).

[8] M. Sūdžius, A. Bastys, K. Jarašiūnas, *Opt. Commun.* **170,** 149 (1999).

[9] M. Sūdžius, V. Gudelis, R. Aleksiejūnas, J. Storasta, K. Jarašiūnas, A. Cola, in: *Proc. SPIE*, Vol. 5024, Eds. S.V. Svechnikov, M.Y. Valakh, SPIE, Washington DC 2003, p. 145.

[10] V.Y. Ivanov, G. Karczewski, M. Sawicki, M. Godlewski, A.R. Omel'chuk, N.V. Zhavoronkov, A.A. Davydov, *Phys. Status Solidi C* **1,** 961 (2004).

[11] D. Verstraeten, J.C. Launay, P. Delaye, D.N. Nguyen, M. Germain, O. Viraphong, P.C. Lemaire, in: *Trends in Optics and Photonics Series*, Vol. 87, Eds. P. Delaye, K. Denz, L. Mager, G. Montemezzani, OSA, Washington DC 2003, p. 159.

[12] H.J. Eichler, P. Günter, D.W. Pohl, *Laser-Induced Dynamic Gratings*, Vol. 50, Springer, Berlin 1986.

[13] M. Godlewski, M. Kaminska, *J. Phys. C* **13,** 6537 (1980).

[14] E. Sorokin, I.T. Sorokina, *Appl. Phys. Lett.* **80,** 3289 (2002).

[15] S. Bhaskar, P.S. Dobal, B.K. Rai, R.S. Katiyar, H.D. Bist, J.-O. Ndap, A. Burger, *Appl. Phys.* **85,** 439 (1999).

[16] E. Gaubas, J. Vaitkus, K. Jarasiunas, *Phys. Status Solidi A* **69,** K87 (1982).

[17] R. Aleksiejunas, M. Sudzius, K. Jarasiunas, *Opt. Commun.* **198,** 115 (2001).